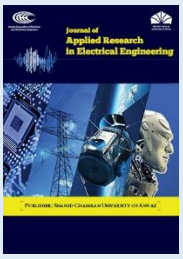
Shahid Chamran University of Ahvaz

Iranian Association of Electrical and Electronics Engineers

Journal of Applied Research in Electrical Engineering

E-ISSN: 2783-2864
P-ISSN: 2717-414X
Homepage: https://jaree.scu.ac.ir/



Research Article

Efficient Coefficient Estimation of Polynomial Phase Signals: A Novel FFT-Free Filtering Method

Seyed Rouhollah Samareh Hashemi [1,*], Fatemeh Hatami [2]

[1] *Fiber Optics group, Institute of Science and High Technology and Environmental Sciences, Graduate University of Advanced Technology, Kerman, Iran*

[2] *Electrical and Computer Engineering Department, Graduate University of Advanced Technology, Kerman, Iran*

** Corresponding Author: sr.hashemi@kgut.ac.ir*

Abstract: The polynomial phase signal (PPS) model is widely utilized in various communication systems, with the estimation of its phase polynomial coefficients being a primary objective for parameter estimation. Noise is a significant source of error in PPS coefficient estimation; therefore, enhancing the signal-to-noise ratio (SNR) of PPSs is crucial for achieving more accurate coefficient estimates. This paper presents a novel filtering algorithm for PPSs that leverages sub-signal filtering and combination techniques. The sub-signal filtering employs a fast, FFT-free frequency estimation method based on phase difference averaging (PDA), de-chirping, and a moving average filter. Following sub-signal filtering, the combination of sub-signals through averaging in overlapping regions further improves the SNR. Also, for selection of optimal sub-signal length, a new optimality criterion is proposed. Theoretical analyses and simulations demonstrate that this algorithm achieves acceptable accuracy with reduced complexity compared to FFT-based methods. Additionally, when estimating the phase polynomial coefficients, the proposed filtering algorithm, combined with phase unwrapping and least-squares estimation, can achieve a mean square error (MSE) that is lower than or equal to that of the superior QML method, while significantly reducing computational complexity.

Keywords: Polynomial phase signal (PPS), polynomial coefficient estimation, filtering algorithm, frequency estimation.

Article history
Received 07 April 2025; Revised 30 December 2025; Accepted 25 February 2026; Published online 10 August 2026.
© 2026 Published by Shahid Chamran University of Ahvaz & Iranian Association of Electrical and Electronics Engineers (IAEEE)

How to cite this article
S. R. Samareh Hashemi, and F. Hatami, " Efficient Coefficient Estimation of Polynomial Phase Signals: A Novel FFT-Free Filtering Method," *J. Appl. Res. Electr. Eng*., vol. 4, no. 2, pp. 242-253, 2025. DOI: https://doi.org/10.22055/jaree.2026.49354.1190

Check for updates

1. INTRODUCTION

A polynomial phase signal (PPS) is a complex signal with constant or nearly constant amplitude and a phase that can be approximated by a polynomial function. In PPS, the primary objective often revolves around estimating the coefficients of the polynomial phase. This estimation is crucial in various domains, including radar signal processing [1][2], sonar systems [3][4], and medical signal processing [5][6]. Synthetic Aperture Radar (SAR) and Inverse Synthetic Aperture Radar (ISAR) signals can be effectively modeled as PPS. Leveraging the estimated parameters from these signals, we can infer critical information such as the speed, acceleration, position, or trajectory of moving targets [7][8]. Another familiar signal that can be estimated as a PPS is the frequency modulated (FM) signal. In the context of parametric estimation for FM signals, polynomial phase modeling is commonly employed [9]-[11]. However, a significant challenge in PPS lies in accurately estimating its polynomial phase coefficients. Over the past few decades, researchers have proposed various estimators, which can be broadly categorized into three main groups: Phase Unwrapping (PU) Estimators, Maximum Likelihood (ML) Estimators and the Phase Differentiation (PD) Techniques.

While PU estimators exhibit low computational complexity, they are sensitive to noise, and their accuracy significantly diminishes as noise level increases [12]. Notably, a specific parameter estimation method for PPS involves employing the spectrum phase unwrapping algorithm, which is effective for certain PPS types known as Strictly Monotonic Polynomial Phase Signals (SMPPS)

[13]. However, when the Signal-to-Noise Ratio (SNR) is low, this method becomes unsuitable for non-SMPPS scenarios due to its reliance on phase differentiation.

The Maximum Likelihood (ML) estimator for polynomial phase signal parameters was initially proposed in the 1960s [14]. While this estimator excels in terms of Mean Square Error (MSE), its computational burden is substantial due to multidimensional searches. To address this challenge, researchers have explored novel approaches aimed at reducing the search space. One such approach leverages the concept of PD. For instance, the High-order Ambiguity Function (HAF) estimator repeatedly employs PD to reduce the order of the phase polynomial. This transformation converts the polynomial into a sinusoid, allowing estimation of the highest-order coefficient via Fourier transform maximization. Subsequent coefficients are estimated iteratively [15]. Another proposed estimator is the HAF product function (PHAF) [16]. PHAF calculates the product of multiple HAF functions. Although more robust to noise than HAF, it comes with increased computational demands. A significant advancement in PPS parameter estimation was the Cubic Phase Function (CPF) estimator [17]. CPF reduces the number of PDs and mitigates noise effects by calculating fewer PDs compared to the HAF approach. Additionally, researchers have introduced the combined CPF-HAF algorithm [18], which requires fewer PDs. However, PD-based estimators exhibit acceptable speed and accuracy but struggle with higher-order PPSs at low SNR.

Yet another estimator for PPS coefficients is the Quasi-Maximum Likelihood (QML) estimator [19][20]. The QML estimator employs a time-frequency transform to estimate instantaneous frequency, determining the time-frequency conversion window length through a search method and quasi-maximum likelihood criterion. QML aims to enhance the accuracy of phase coefficient estimation under low SNR conditions [21].

In all PPS estimation methods, noise profoundly impacts the quality of PPS coefficient estimation; so, in this study, our goal has been to develop a method for PPS filtering and noise reduction. Noise filtering algorithms have been developed in various areas of signal processing [22]-[24]. After noise reduction, any of the PPS estimation methods can be employed with lower SNR threshold; beyond which the MSE of the estimator reaches close to the Cramer-Rao Lower Bound (CRLB). Due to the critical importance of algorithmic speed, our objective has been to achieve low computational complexity. Consequently, we have avoided the use of the Discrete Fourier Transform (DFT), and all filtering operations within the algorithm consist solely of simple multiplication, addition, or averaging. Our algorithm is based on dividing the signal into short-length sub-signals, filtering the sub-signals by an innovative PD-based FFT-free method, and finally combining them by averaging over sub-signals. By segmenting PPS into short-length sub-signals, each sub-signal approximates a constant frequency signal. This allows us to estimate the frequency using a technique named as Phase Difference Averaging (PDA), rather than employing the fast Fourier Transform (FFT). In the filtering step, the phase slope (frequency) of each sub-signal is first estimated using the PDA method. Subsequently, using the estimated frequency, the frequency of the sub-signal is set to zero through a de-sloping (or de-chirping) operation. Once the frequency content of the sub-signal is centered around zero, noise reduction can be achieved using a simple moving average filter (MAF). After filtering, the original frequency of the sub-signal is restored through a reverse operation named re-sloping. By implementing these four steps—PDA, de-sloping, MAF, and re-sloping—we obtain a filtered version of each sub-signal. Finally, the filtered sub-signals are combined through an averaging process to produce the filtered PPS.

To determine the optimal length of the sub-signals, a one-dimensional search approach is employed. However, in contrast to the Quasi-Maximum Likelihood (QML) method, we have developed a novel optimality criterion that mitigates noise-induced effects.

Simulations show that this algorithm can effectively mitigate noise-induced challenges during coefficient estimation, ultimately enhancing the accuracy of PPS phase coefficient estimation comparable to the superior method of QML, but with lower computational burden.This paper is organized as follows: Section 2 is a theoretical background and involves the introduction of PPS and frequency estimation of a linear phase PPS. Section 3 describes our proposed algorithm, and Section 4 presents simulation and results. Finally, Section 5 provides the conclusions.

2. THEORETICAL BACKGROUND

2.1. PPS Model

A PPS signal of length N can be modeled as:

$$s(n) = exp(\, j\, \varphi(n)\,), \quad n = -\mathrm{N}/2, \ldots, \mathrm{N}/2 - 1$$
$$\varphi(n) = a_0 + a_1(n\Delta t) + a_2(n\Delta t)^2 + \cdots + a_P(n\Delta t)^P = \sum_{i=0}^{P} a_i(n\Delta t)^i \quad (1)$$

Where $\varphi(n)$ is the polynomial phase, a_i is the i^{th} polynomial coefficient and Δt is the sampling interval. Without loss of generality, the amplitude of PPS is set to 1. The noisy version of PPS is considered as:

$$x(n) = s(n) + w(n) \quad (2)$$

Where $w(n)$ is a noise with zero mean and variance σ^2.

2.2. Estimation of the phase slope (frequency) of a liner phase PPS

Since the key step of the proposed algorithm is dividing the PPS into sections with approximately linear phase, the estimation of the frequency of a linear phase signal in the algorithm is critical. The conventional method for estimating the frequency of a linear phase signal is the maximization of the Fourier Transform [25]. However, in this research, we used the PD method instead of the Fourier transform, as its lower computational load with acceptable accuracy. If the signal $x(n)$ is considered as (2) and $s(n)$ is a linear phase PPS as:

$$s(n) = e^{jan} \quad (3)$$

The complex number $\alpha = e^{ja}$, which involves the phase slope a, can be estimated by a phase difference (PD) operation according to:

$$p(n) = s(n) \times s^*(n-1) = e^{jan} \times e^{-ja(n-1)} = e^{ja} \quad (4)$$

For a noisy PPS, the PD operation can be expressed as:

$$p(n) = [e^{jan} + w(n)] \times [e^{ja(n-1)} + w(n-1)]^* \quad (5)$$

$$= e^{ja} + e^{jan}w^*(n-1) + e^{-ja(n-1)}\,w(n) + w(n)w^*(n-1)$$

By considering (5), we can conclude that for estimating e^{ja}, an averaging operation over all samples of $p(n)$ will increase the estimation accuracy. This operation is named phase difference averaging (PDA):

$$Ave(p(n)) = \frac{1}{\mathrm{N}-1}\sum_{n=-\frac{N}{2}+1}^{\frac{\mathrm{N}}{2}-1} p(n) = e^{ja} + \frac{1}{\mathrm{N}-1}\sum_{n=-\frac{N}{2}+1}^{\frac{\mathrm{N}}{2}-1}\left[w(n)e^{-ja(n-1)} + w^*(n-1)e^{jan} + w(n)w^*(n-1)\right] \quad (6)$$

Where $Ave(.)$ is the averaging operator. It is worth noting that by calculating the expectation of the right-hand side of (6) and supposing that the noise samples are uncorrelated, we can conclude that this estimation is unbiased:

$$E\left(Ave(p(n))\right) = e^{ja} \quad (7)$$

Where $E(.)$ is the expectation operator. Also, the variance of the PDA can be obtained as (see Appendix A):

$$var\left(Ave(p(n))\right) = \frac{\sigma^4 + 2\sigma^2}{\mathrm{N}-1} \quad (8)$$

The two parameters that affect the accuracy of the phase slope estimation by PDA are the noise variance and the signal length. Next (in section 4.1), we will show that the estimation error of (8) is acceptable in moderate noise conditions compared to FFT-based method.

3. PROPOSED ALGORITHM

3.1. Algorithm Steps

Building upon the concepts introduced in the previous sections, we outline the implementation steps of our proposed algorithm as below.

Segmentation: The input signal (PPS) of length N is divided into M sub-signals of length L. Each sub-signal overlaps with the adjacent sub-signal at L_1 samples (as depicted in Fig. 1). After segmentation, it is assumed that the length of each sub-signal is short enough such that the phase of each sub-signal is approximately linear. The k^{th}sub-signal $x_k(n)$ can be expressed as:

$$x_k(n) = x(n)\ for\ \ n_{1k} \le n \le n_{2k}\ \ where:$$
$$n_{1k} = -\frac{N}{2} + (k-1)L_1,\ \ n_{2k} = n_{1k} + L - 1, and \quad (9)$$
$$k = 1,2,\dots,M$$

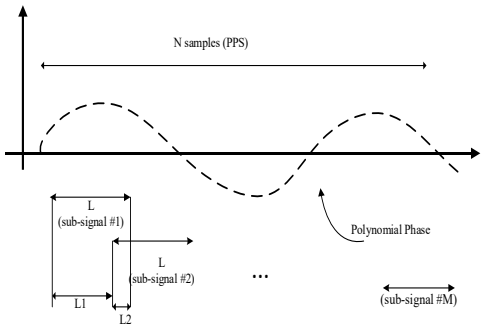


Fig. 1: Dividing the signal $x(n)$ into M overlapping sub-signals.

Phase Slope Estimation: When $x(n)$is divided into sub-signals, the PDA method described in 2.2 is used to obtain the phase slope:

$$\widehat{\alpha_k} = Ave(p_k(n)) = \frac{1}{L-1}\sum_{n=n_{1k}+1}^{n_{2k}} p_k(n) \quad (10)$$
$$where: p_k(n) = x_k(n)\,x_k{}^*(n-1),\ \ n_{1k} \le n \le n_{2k}$$

$\widehat{\alpha_k}$ is the estimation of $\alpha_k = e^{ja_k}$ and a_k is the phase slope of the k[th] sub-signal.

De-Sloping: In this step, using the estimated $\widehat{\alpha_k}$, the phase slope of the sub-signal is set to zero. The goal of de-sloping is to obtain a narrowband low-pass signal that can be filtered by a simple averaging filter. De-sloping is performed as:

$$d_k(n) = x_k(n) \times \widehat{\alpha_k}^{(-n)}\ \ ,\ \ n_{1k} \le n \le n_{2k} \quad (11)$$

Where $d_k(n)$ is the k'th de-sloped sub-signal. In the noise free conditions, the result of de-sloping of a linear phase PPS is a pure dc (constant) signal. In real conditions that the noise is present and the sub-signal is not a pure fixed-frequency signal, the result of de-sloping is a noisy narrowband low-pass signal.

Noise Filtering: Since the frequency of the sub-signal after de-sloping is concentrated around zero, an averaging over a sliding window can be used to filter the de-sloped sub-signal:

$$y_k(n) = MAF\{d_k(n)\} = \frac{1}{W}\sum_{m=\left\lfloor -\frac{W-1}{2}\right\rfloor}^{\left\lfloor\frac{W-1}{2}\right\rfloor} d_k(n-m) \quad (12)$$

Where $y_k(n)$ is the filtered de-sloped sub-signal, MAF stands for moving average filter and W is the length of the averaging window.

Re-sloping: After noise reduction, the removed phase of the sub-signal should be returned, and it is the reverse of the de-sloping:

$$z_k(n) = y_k(n) \times \widehat{\alpha_k}^{(n)}\ \ ,\ \ n_{1k} \le n \le n_{2k} \quad (13)$$

Where $z_k(n)$ is the re-sloped filtered sub-signal and it is a noise reduced version of the k'th sub-signal $x_k(n)$.

Combination: After filtering sub-signals, it is necessary to combine them to have the complete filtered PPS. For this purpose, each of $z_k(n)$ is placed in the k'th row of a "combination matrix". If we consider the (k,n) element of the combination matrix as $\Pi(k,n)$, then we have:

$$\Pi(k,n) = \begin{cases} z_k(n) & n_{1k} \le n \le n_{2k} \\ 0 & elsewhere \end{cases} \quad (14)$$

The matrix Π has dimensions M×N and in each row, the filtered sub-signal is in its corresponding place, and other entries are zeros (As seen in Fig. 2). Finally, an averaging operation is performed on the columns of the combination matrix. Here, in addition to the filtering each sub-signal, we have an averaging operation on different sub-signals, which is a filtering over all sub-signals. Another method for combining filtered sub-signals is to use an accumulator of length N. The filtered sub-signals after zero-padding (the rows of the combination matrix) are accumulated by the accumulator one after another. Finally, the scaled version of the accumulator will be the filtered PPS. The action of the Accumulator is like as a summation on the columns of the combination matrix.

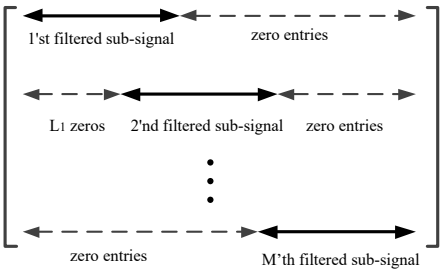


Fig. 2: combination matrix

3.2. Sub-signal Length and Overlap

At the beginning of the proposed algorithm, we should select two parameters: the length of the sub-signal (L) and the overlapping ratio witch is defined as:

$$O = \frac{L_2}{L} \tag{15}$$

where L_2 is the length of the overlap between adjacent sub-signals. For selecting the overlap ratio, it is showed in the following (section 4.3) that we have a trade-off between the accuracy and the computational load; but, for a rule of thumb, an overlap ratio about 0.5 or higher is sufficient. The selection of the length of the sub-signal is important, so we developed a search method to optimize the parameter L. In this method, we repeat the filtering algorithm for several sub-signal lengths and finally select the best result using an optimality criterion, that is:

$$E(L) = \frac{1}{N}\sum_{n=-\frac{N}{2}}^{\left(\frac{N}{2}\right)-1}\left|\left|x_f^{(L)}(n)\right| - \mu_f^{(L)}\right|^2 \tag{16}$$

$$where: \quad \mu_f^{(L)} = \frac{1}{N}\sum_{n=-\frac{N}{2}}^{\left(\frac{N}{2}\right)-1}\left|x_f^{(L)}(n)\right|$$

Here, $x_f^{(L)}(n)$ is the filtered signal with sub-signal length L and $\mu_f^{(L)}$ is the mean of the amplitude of $x_f^{(L)}(n)$. It is obvious that the above criterion is the variance of the amplitude of the filtered signal. In designing this criterion, we considered the fact that the amplitude of the noiseless PPS is constant. So, during the filtering process, the sub-signal length that results in the minimum variance of the amplitude of the filtered signal is selected as the optimal L. the effectiveness of this criterion was satisfied by simulations. Therefore, the most appropriate sub-signal length, L_o, is chosen as:

$$L_o = \arg\min_L E(L) \tag{17}$$

It is worth noting that in QML, the most appropriate short-time Fourier transform (STFT) length is selected by (18):

$$L_o = \arg\max_L \left|\sum_{n=-N/2}^{(N/2)-1} x_{QML}^{(L)}(n)x^*(n)\right| \tag{18}$$

where $x_{QML}^{(L)}(n)$ is the estimated PPS by the QML algorithm using the STFT length of L. However, if we use (18) in our algorithm, the selected sub-signal length leads to a filtered signal $x_f^{(L)}(n)$ that follows the noisy signal $x(n)$ to some extent. More clearly, if we rewrite (18) in terms of the amplitude and phase of two signals, we will have:

$$L_o = \arg\max_L \left|\sum_{n=-N/2}^{(N/2)-1} \left|x_{QML}^{(L)}(n)\right||x(n)|e^{j[\measuredangle x_{QML}^{(L)}(n) - \measuredangle x(n)]}\right| \tag{19}$$

where $\measuredangle x_{QML}^{(L)}(n)$ and $\measuredangle x(n)$ are the phases of $x_{QML}^{(L)}(n)$ and $x(n)$. It is clearly seen from (19) that if the output signal phase of the QML algorithm is close to the initial signal phase, the value of the above expression is maximized, that is, this criterion seeks to reduce the distance of the output signal phase from the input signal phase. But, using this criterion in our filtering algorithm leads to the selection of short sub-signal lengths and so the phase of the output signal will follow the phase of the noisy signal. Simulations (section 4.2) show the better results of the proposed criterion of (17) compared to the QML criterion of (18). Fig. 3 shows the flowchart of the algorithm.

3.3. Computational Complexity

The necessary calculations in each step of the proposed algorithm are given in Table 1.

In the last column of Table 1, L is the sub-signal length and M is the number of sub-signals. W is the moving average length and we know: $W \ll L$.

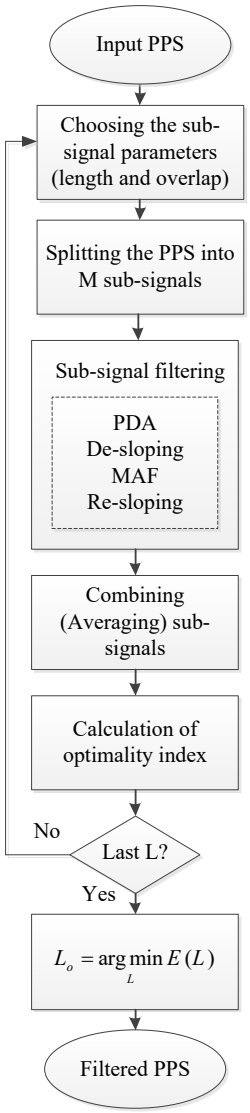


Fig. 3: Flowchart of the proposed filtering algorithm

Table 1: Necessary calculations in the proposed algorithm

algorithm steps	Calculations for each sub-signal	Calculations for all sub-signals
Phase difference	L-1 complex multiplications	(L-1)M complex multiplications
Averaging on $p_k(n)$	L-2 complex additions	(L-2)M complex additions
De-slope	L complex multiplications	L×M complex multiplications
Filtering	W×L complex additions and L multiplications	W×L×M complex additions and M×L multiplications
Re-slope	L complex multiplications	L×M complex multiplications
Sub-signals combination	L complex additions	L × (M − 1) complex additions and N multiplications

So, the computational complexity of the algorithm for each sub-signal length is $O(ML)$. To compare the value of ML with the number of PPS samples N, we have (See Fig. 1):

$$\begin{aligned} N = ML_1 + L_2 &= M(L - L_2) + L_2 \\ &= ML - (M-1)L_2 \\ &= ML - (M-1)QL \\ &\cong ML(1-Q) \end{aligned} \qquad (20)$$

$$\Longrightarrow ML \cong \frac{N}{1-Q}$$

Therefore, the number of operations of the algorithm depend the overlap ratio. For example, if we choose $Q = 0.5$, according to (20) we have $LM \cong 2N$, then the computational complexity will be $O(N)$; while, if we used FFT in the algorithm, in each sub-signal a complex FFT of length L or larger (in the case of zero-padding) would be needed, so the number of complex operations would be $O(MLlog_2L)$.

4. SIMULATIONS

4.1. Filtering a Linear Phase Signal

For evaluation of the proposed PDA algorithm for estimating the phase slope of a linear phase PPS, we performed simulations and analyzed the results. First, we considered a signal like (3) with $a = 1$ and $N = 16$. We added complex Gaussian noise to reach the desired SNR. Then we applied PDA to estimate e^{ja}. The SNR is changed from -15dB to 15dB with 3dB increments and in each case, we repeated the simulation 1000 times and finally the mean square error (MSE) of the estimation process is calculated. Moreover, we calculated the theoretical MSE of the estimation (See appendix A). In Fig. 4 the result of the simulation and theoretical evaluation of the MSE is depicted vs. signal SNR. As seen, these values coincide. For comparison, we estimated the phase slope (frequency) of the signal using the common method of maximizing the FFT of the signal and the MSE of this estimation is also depicted in Fig. 4. As seen, at low SNRs, the FFT method outperforms the PDA. At high SNRs, the PDA results are better. This is because the number of frequency divisions, here 16, in the FFT method for estimating the signal frequency is limited, and so, increasing the SNR doesn't result in decreasing MSE. For overcoming this limitation, it is necessary to increase the frequency division by zero padding. For example, the result of zero-padding the signal to 1024 and then using the FFT method is depicted in Fig. 4. In this case, the MSE at $SNR > 3dB$ has reached very close to the Cramer-Raw lower bound (CRLB), albeit by 160 times more operations compared to FFT of length 16.

PPS estimation methods generally are good at high SNRs and fail at very low SNRs, but mid SNRs ($-5dB \leq SNR \leq 5dB$) are very important and challenging. Most of PPS estimation methods have the "knee" of the MSE curve in the mid SNR range. As seen in Fig. 4, the performances of the PDA and FFT methods are close and comparable in this range, noting that the operations of the PDA are less. This is the point that rationalized the use of PDA in PPS filtering and estimation.

In the proposed filtering method, PDA is applied on the sub-signals, and the length of sub-signals shouldn't be so long and is usually between 8 and 32. In another simulation, the MSE of the output of two phase slope estimation methods PDA and FFT is calculated for lengths 8 and 32. In this simulation, we selected a high frequency signal as $a = 0.9\pi$. Fig. 5 shows the result. As seen, in the case $N = 8$, two algorithms have approximately the same performance in mid SNRs. At $N = 32$, although the FFT error is lower in some SNRs, the higher speed of the PDA method still justifies the use of this method. In general, the longer the sub-signal length, the greater the distance between the FFT error and the PDA error

4.2. Filtering High-order PPS

In the second simulation, we used a PPS of length N=256 with a polynomial phase of order 7. This PPS is used earlier in [21]. The polynomial coefficients are listed in Table 2. Gaussian noise is added to the PPS to have the desired SNR. Then, the noisy PPS is filtered by the proposed algorithm. In Fig. 6(a) the real and imaginary parts of the pure signal (without noise), noisy signal with SNR=-3dB and the filtered signal is shown. As seen, although the low SNR of -3dB, the algorithm could has reduced the noise significantly. In Fig. 6(b) the absolute value and unwrapped phase of the original, noisy and filtered signal is shown. Since the phase of the PPS carries the information of the signal, it is important to have a noise-free phase. Clearly, the proposed algorithm has reduced the noise, so, the wrong jumps in the unwrapping process are eliminated compared to the unwrapped phase of the noisy signal.

In Fig. 7, the output of the algorithm using the QML criterion of sub-signal length discussed in (18) is depicted. Compared to Fig. 6, it is obvious that in this case the filtered signal is more affected by the noise because the criterion of (18) imposed short sub-signal lengths and leads to the effect of noise following.

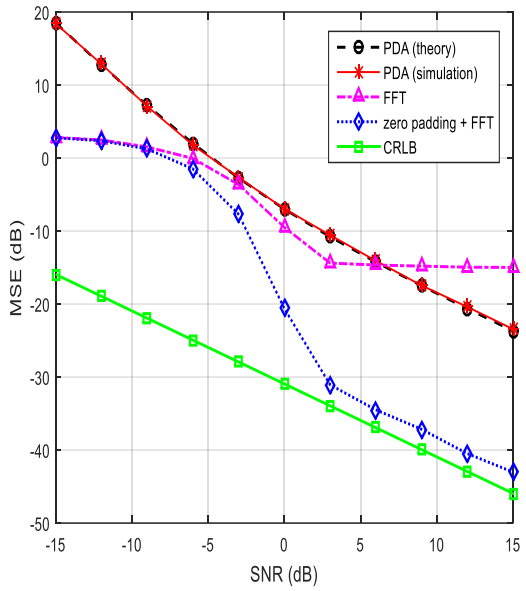


Fig. 4: MSE vs. SNR for estimation of the phase slope of a linear phase PPS.

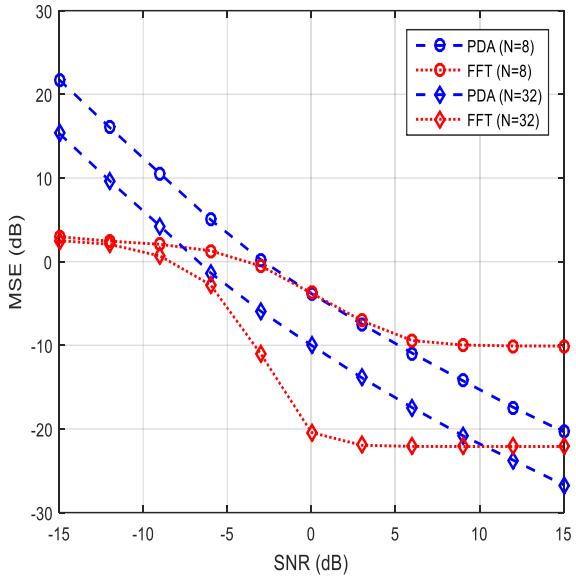


Fig. 5: MSE vs. SNR for estimation of the phase slope of a linear phase PPS for N=8 and N=32.

In the next simulation, a radar scenario is considered. In this scenario, the signal of a moving target and clutter plus noise is simulated and filtered by the proposed algorithm.

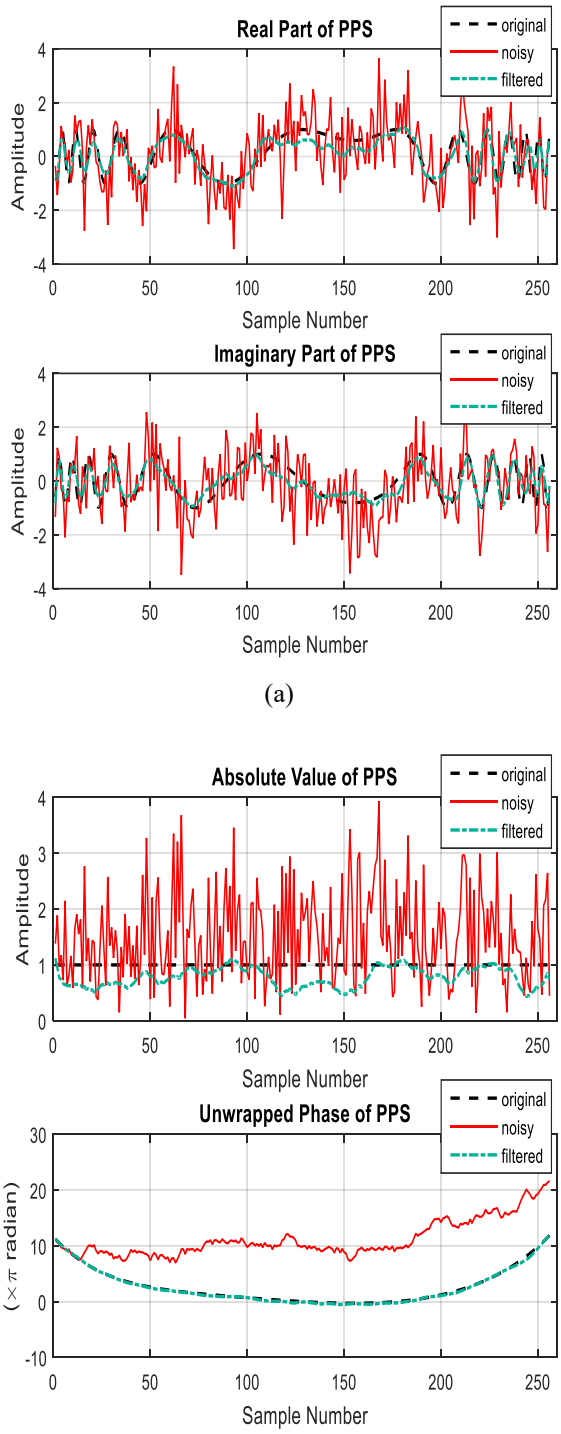
The baseband signal of the radar is modelled as:

$$x(n) = \sigma_t \exp\left(-j\frac{4\pi f_0}{c}R(n)\right) + \sigma_c + w(n) \qquad (21)$$

Where σ_t is the complex reflectivity of the moving target, f_0 is the carrier frequency, c is the speed of light, $R(n)$ is the range distance of moving target at time sample n, σ_c is the complex reflectivity of clutter and $w(n)$ is the noise. The range distance of the moving target assuming an accelerated movement in x and y direction is:

Table 2: coefficients of the phase polynomial for sampling interval $\Delta t = 0.0078$

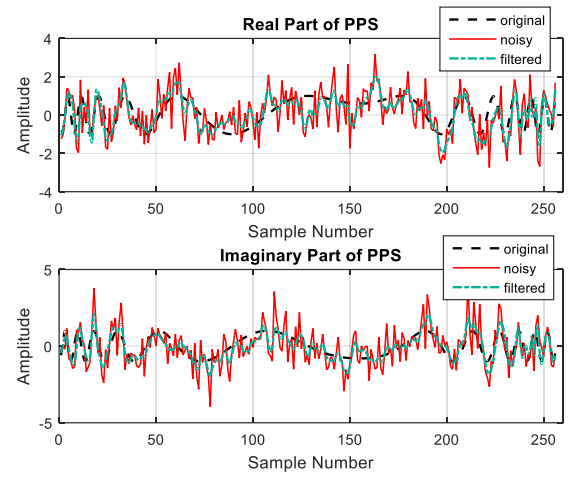
Coefficient	a_0	a_1	a_2	a_3	a_4	a_5	a_6	a_7
Value	0	−8	12	21	13	−14	12	2



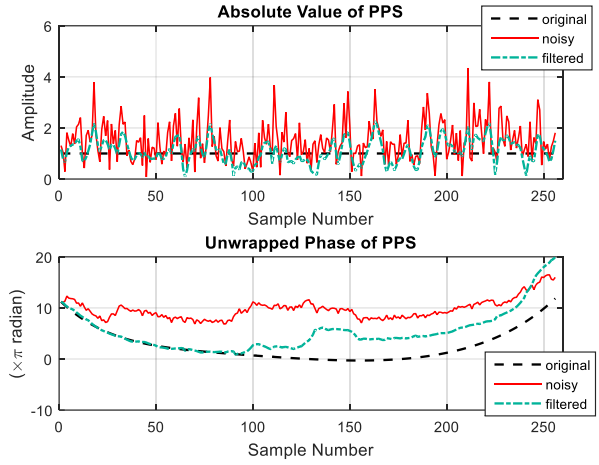
(a)

(b)

Fig. 6: The results of the proposed filtering algorithm for a PPS with SNR=-3dB (a) real and imaginary parts, (b) absolute values and unwrapped phases



(a)



(b)

Fig. 7: The results of the proposed filtering algorithm for a PPS with SNR=-3dB and the sub-signal length criterion of (18) (a) real and imaginary parts, (b) absolute values and unwrapped phases

$$R(n) = \left(h^2 + \left(x_0 + v_x(n\Delta t) + \frac{1}{2}a_x(n\Delta t)^2\right)^2 + \left(y_0 + v_y(n\Delta t) + \frac{1}{2}a_y(n\Delta t)^2\right)^2\right)^{\frac{1}{2}} \quad (22)$$

It is assumed that the radar is at the position $(0,0,h)$ and the moving target is at the position $(x_0, y_0, 0)$ at $n = 0$. v_x, v_y, a_x and a_y are velocities and accelerations of the moving target in x and y directions respectively and Δt is the sampling interval. By substituting (22) in (21) and ignoring the noise, we will have a signal that has an almost constant amplitude and variable phase. The phase can be expanded as a polynomial, although is not a pure polynomial. We used these parameters for our simulation: $h = 30m$, $x_0 = 500m$, $y_0 = 500m$, $v_x = -15m/s$, $v_y = 15m/s$, $a_x = -1\,m/s^2$, $a_y = 5\,m/s^2$, $\Delta t = 1ms$, $f_0 = 10GHz$ and $\sigma_t = 1$. The signal to clutter ratio (SCR) is adjusted to 10dB and SNR is adjusted to desired values. The absolute value of σ_c is picked from a Rayleigh distribution and its phase from a uniform distribution. Simulation is done for 512 samples from -256 to 255. In Fig. 8 a plot of the amplitude, unwrapped phase, real part and imaginary part of the noise-and-clutter-free signal along with the noisy and filtered signal using the proposed algorithm at SNR=-3dB is depicted. As seen, the quality of the filtered signal is satisfactory compared with the noisy signal.

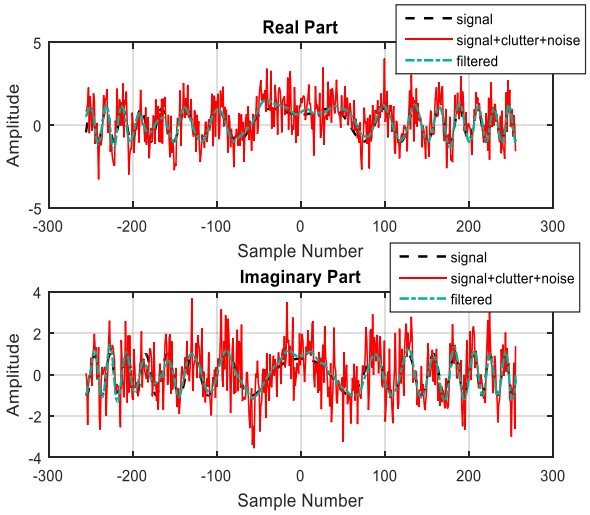
Fig. 9 shows the MSE of the real and imaginary parts of the received and filtered signals vs. SNR. For example, The MSE of the real part for filtered signal is defined as:

$$MSE = E\{(real\{x_r(n) - x_f(n)\})^2\} \quad (23)$$

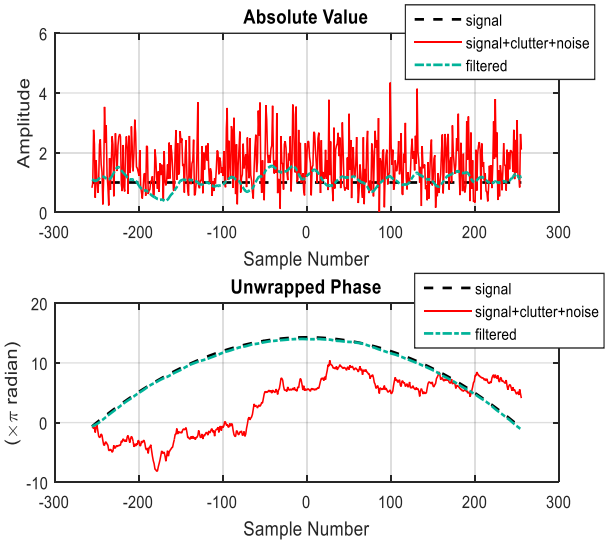
Where $x_r(n)$ is the noise-free received signal from the moving target and $x_f(n)$ is the filtered signal. MSE is calculated by averaging over 1000 trials. Other MSEs are calculated similarly. Clearly, the proposed algorithm has decreased the MSE several decibels.

4.3. PPS Phase Coefficient Estimation

Although the basic purpose of the proposed algorithm is noise cancellation, but we can use this algorithm prior to coefficient estimation algorithms. In this simulation, we analysed the utilization of the proposed filtering algorithm for estimating the phase parameters of a PPS. We considered the PPS of Table 2.



(a)



(b)

Fig. 8: The results of the proposed filtering algorithm for the radar signal at SNR=-3dB: (a) real and imaginary parts, (b) absolute values and unwrapped phases

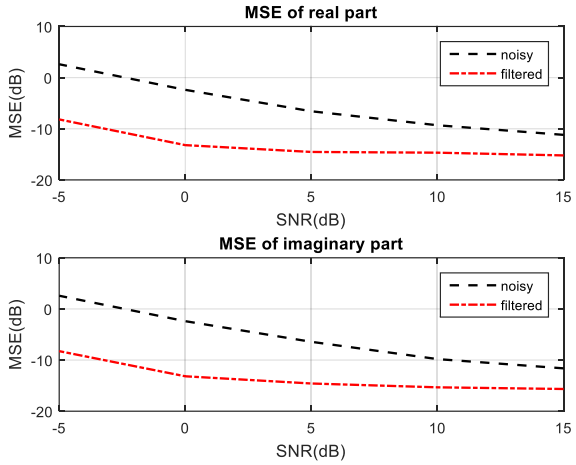


Fig. 9: The MSE of the real in imaginary parts of the noisy and filtered signals in radar scenario

White Gaussian noise is added to achieve the desired SNR. For each SNR, we employed our proposed filtering algorithm on the noisy PPS. The sub-signal length is set to 8, 16, 32 and 64 with an overlap of 0.9 and we selected the best length based on the optimality criterion of (17). Subsequently, we applied the basic phase unwrapping algorithm followed by the least-squares polynomial coefficient estimation [26]. For comparison, we also evaluated the superior QML algorithm for estimating the PPS coefficients. Both algorithms incorporate a refinement step [27].

Fig. 8 illustrates the estimation results for the last coefficient (a_7). To obtain this curves, we computed the MSE of a_7 estimation for 10000 trials across an SNR range of -5 dB to 15 dB with 5 dB steps.

As can be seen, the proposed PDA filtering algorithm followed by simple phase unwrapping and least squares estimation, achieved an MSE that is either less than or equal to that of the QML algorithm.

The average execution time for each evaluation of the proposed algorithm and the QML algorithm is given in Table 3. Our implementations were carried out using MATLAB software version R2017a on a computer with a 1.8 GHz CPU, 4 GB RAM, and Windows 10 operating system. Notably, the proposed algorithm demonstrates shorter execution time despite of the high overlap ratio of 0.9.

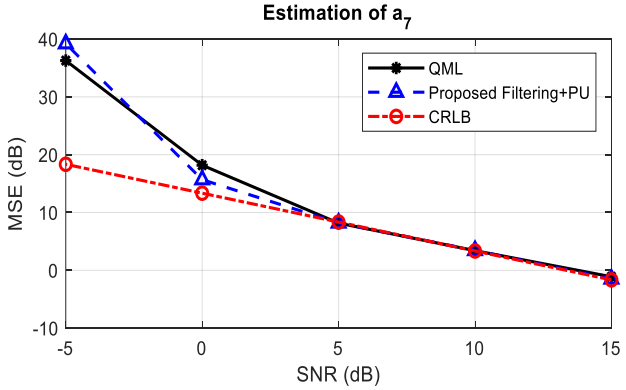


Fig. 10: MSE of estimation using the proposed filtering algorithm followed by basic phase unwrapping and least-squares estimation compared to the QML algorithm.

Table 3: Average execution time for the proposed algorithm and the QML algorithm

Algorithm	Average execution time
Proposed filtering algorithm followed by phase unwrapping and least squares estimation	43.7ms
QML algorithm	88.3ms

In another simulation, a 10 order polynomial phase is used in the simulation. In each realization of the signal, the coefficients of the phase polynomial are generated as uniform distributed random numbers in the range [-10,10] and Δt is selected as 8ms. Other steps of the simulation are like the previous simulation. In Fig. 11 the MSE of the last four coefficients vs. SNR are showed. Here too, the performance of the proposed filtering algorithm followed by phase unwrapping and least square estimation is comparable to QML.

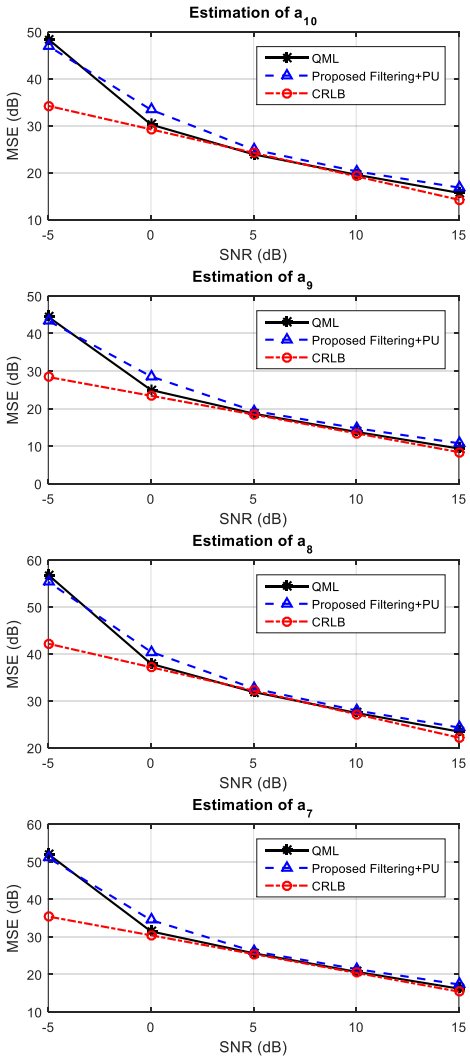


Fig. 11: MSE of estimation using the proposed filtering algorithm followed by basic phase unwrapping and least-squares estimation compared to the QML algorithm for PPS of order 10 and Gaussian noise

For evaluating the performance of the proposed algorithm with different noise, the simulation of the previous 10 order PPS is done, but this time with Gaussian and spike noise together. The spike noise is simulated with desired amplitude and uniform distributed phase. The spacing between two successive spikes is uniformly selected in the range [12,20] samples. A realization of the real and imaginary parts of the noisy signal with Gaussian noise variance $\sigma^2 = 0.0316$ and spike noise of amplitude 2 is depicted in Fig. 11. As seen, the proposed method has eliminated the powerful spikes.

In Fig. 13 the MSE of the last 4 coefficients of the phase polynomial is shown. In this simulation, the spike amplitude is 1 and the CRLB is calculated considering only the Gaussian noise. As seen, the performance of the proposed method is still comparable to QML.

4.4. Overlap Ratio

In the proposed algorithm, one of the parameters that must be specified and is relevant to the accuracy and speed of the algorithm is the overlap ratio between adjacent sub-signals. Here is a simulation to investigate this issue. In this simulation, we applied the proposed algorithm for estimation PPS coefficients like section 4.3 and the effect of increasing the overlap ratio from 0.3 to 0.9 on the average execution time of the proposed algorithm is investigated. In Fig. 8(a), the average execution time of the proposed algorithm at SNR=0dB is plotted for different overlaps. This figure shows a decrease in speed with an increase in the overlap ratio.

In the above simulation, we also calculated the distance of the MSE error of the estimation to the CRLB vs. the overlap ratio. This distance is a measure of the accuracy of the algorithm and is depicted in Fig. 8(b). The general trend of this graph shows the increase in accuracy with increasing the overlap ratio. So, we can conclude that in setting the overlap ratio we have a trade-off between the speed and the accuracy, but as seen, an overlap ratio above 0.5 is satisfactory.

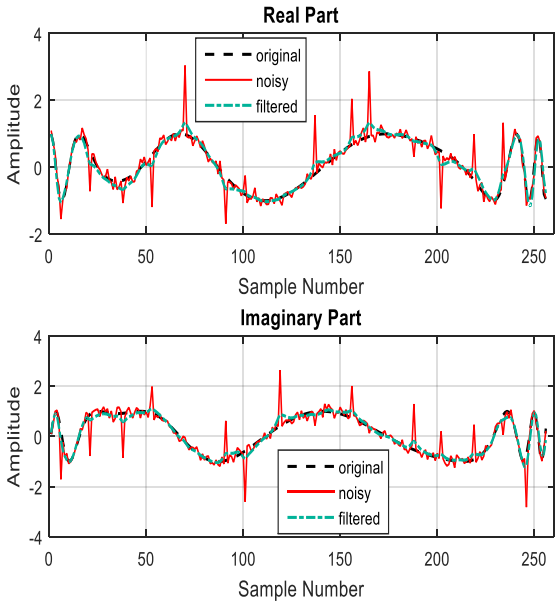


Fig. 12: Real and imaginary parts of the noise-free, noisy (Gaussian+spike), and filtered PPS of order 10

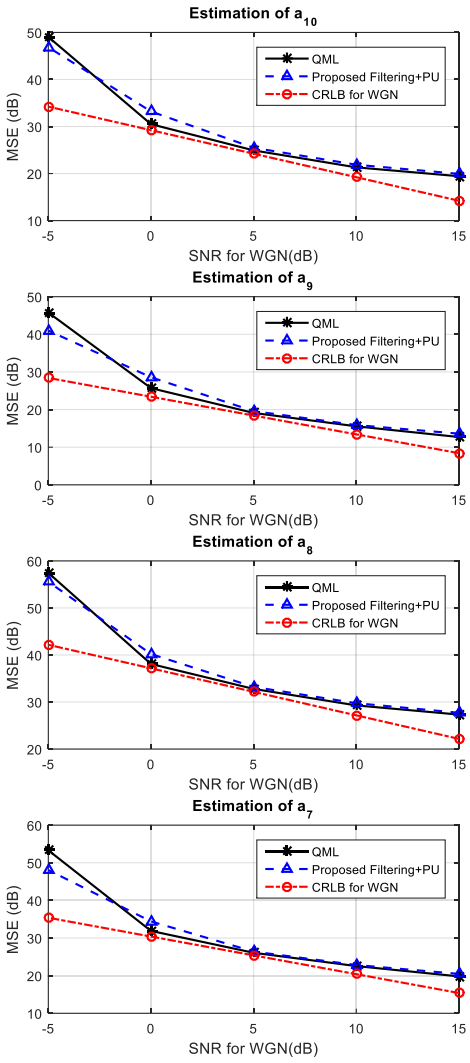


Fig. 13: MSE of estimation using the proposed filtering algorithm followed by basic phase unwrapping and least-squares estimation compared to the QML algorithm for PPS of order 10 with Gaussian along with spike noise

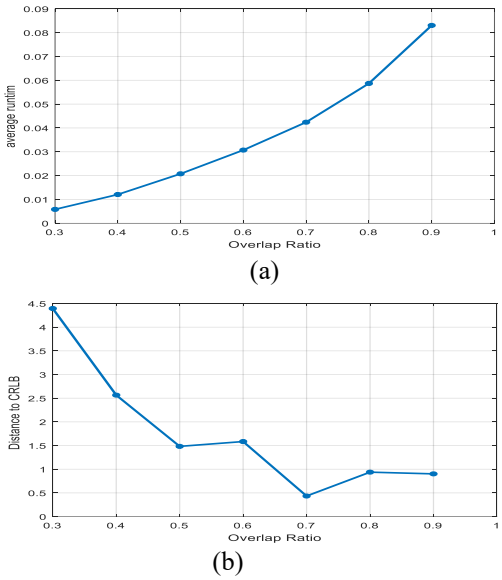


Fig. 14: (a) Investigating the effect of different overlap ratios on the speed of the proposed algorithm, (b) Investigating the effect of different overlap ratios on the accuracy of the proposed algorithm.

5. CONCLUSIONS

In this research, we proposed a filtering algorithm for polynomial phase signals by dividing the signal into sub-signals of approximately linear phase and filtering them through an inter-sub-signal and intra-sub-signal averaging processes. Our aim was to reduce computational complexity as much as possible; therefore, we avoided using the DFT for filtering sub-signals in the frequency domain. Instead, we employed an innovative filtering approach utilizing PDA, de-sloping, MAF, and re-sloping techniques.

To determine the optimal sub-signal length, we introduced a criterion that outperforms the QML criterion. Analyses and simulations demonstrate that our filtering algorithm yields results comparable to those of FFT-based methods, while requiring lower computational resources. Based on our findings, this filtering process is suitable for the general use of noise reduction and also for preparing polynomial phase signals for phase coefficient estimation. The proposed algorithm has several advantages, including low complexity, flexibility in selecting sub-signal overlap (allowing a trade-off between accuracy and speed), no reliance on FFT, and acceptable performance.

Acknowledgment

This research has been supported by the Institute of Science and High Technology and Environmental Sciences, Graduate University of Advanced Technology (Kemran-Iran) under grant number of 97/1981.

Appendix A.

In this appendix, we want to calculate the variance of the PDA operation. According to (6):

$$var\{Ave(p(n))\} =$$

$$var\left\{e^{ja} + \frac{1}{\mathrm{N}-1}\sum_{n=-\frac{N}{2}+1}^{\frac{\mathrm{N}}{2}-1}\left[w(n)e^{-ja(n-1)} + w^*(n-1)e^{jan} + w(n)w^*(n-1)\right]\right\}$$

$$= \frac{1}{(\mathrm{N}-1)^2}E\left\{\sum_{n=-\frac{\mathrm{N}}{2}+1}^{\frac{\mathrm{N}}{2}-1}\sum_{m=-\frac{\mathrm{N}}{2}+1}^{\frac{\mathrm{N}}{2}-1}\left(w(n)e^{-ja(n-1)} + w^*(n-1)e^{jan} + w(n)w^*(n-1)\right)\left(w^*(m)e^{ja(m-1)} + w(m-1)e^{-jam} + w^*(m)w(m-1)\right)\right\}$$

$$= \frac{1}{(\mathrm{N}-1)^2}\sum_{n=-\frac{\mathrm{N}}{2}+1}^{\frac{\mathrm{N}}{2}-1}\sum_{m=-\frac{\mathrm{N}}{2}+1}^{\frac{\mathrm{N}}{2}-1} E\{w(n)e^{-ja(n-1)}w^*(m)e^{ja(m-1)}\}$$

$$+ E\{w(n)e^{-ja(n-1)}w(m-1)e^{-jam}\} +$$

$$E\{w(n)e^{-ja(n-1)}w^*(m)w(m-1)\}$$

$$+ E\{w^*(n-1)e^{jan}w^*(m)e^{ja(m-1)}\}$$

$$+ E\{w^*(n-1)e^{jan}w(m-1)e^{-jam}\} +$$

$$E\{w^*(n-1)e^{jan}w^*(m)w(m-1)\}$$

$$+ E\{w(n)w^*(n-1)w^*(m)e^{ja(m-1)}\}$$

$$+ E\{w(n)w^*(n-1)w(m-1)e^{-jam}\}$$

$$+E\{w(n)w^*(n-1)w^*(m)w(m-1)\}$$

$$= \frac{1}{(\mathrm{N}-1)^2}(2(\mathrm{N}-1)\sigma^2 + (\mathrm{N}-1)\sigma^4)$$

$$= \frac{\sigma^4 + 2\sigma^2}{\mathrm{N}-1}$$

REFERENCES

[1] Y. Zhang, M. G. Amin, and G. J. Frazer, "High-resolution time–frequency distributions for manoeuvring target detection in over-the-horizon radars," *IEE Proceedings-Radar, Sonar and Navigation,* vol. 150, no. 4, pp. 299-304, 2003.

[2] J. J. Sharma, C. H. Gierull, and M. J. Collins, "The influence of target acceleration on velocity estimation in dual-channel SAR-GMTI," *IEEE Transactions on Geoscience and Remote Sensing,* vol. 44, no. 1, pp. 134-147, 2005.

[3] R. F. Brcich and A. M. Zoubir, "The use of the DPT in passive acoustic aircraft flight parameter estimation," in *TENCON'97 Brisbane-Australia. Proceedings of IEEE TENCON'97. IEEE Region 10 Annual Conference. Speech and Image Technologies for Computing and Telecommunications (Cat. No. 97CH36162)*, 1997, vol. 2, pp. 819-822: IEEE.

[4] R. Pfeil, M. Pichler, S. Schuster, and F. Hammer, "Robust acoustic positioning for safety applications in underground mining," *IEEE Transactions on Instrumentation and Measurement,* vol. 64, no. 11, pp. 2876-2888, 2015.

[5] P. Mirzaei, G. Azemi, N. Japaridze, and B. Boashash, "Surrogate data test for nonlinearity of EEG signals: A newborn EEG burst suppression case study," *Digital Signal Processing,* vol. 70, pp. 30-38, 2017.

[6] B. J. Roach and D. H. Mathalon, "Event-related EEG time-frequency analysis: an overview of measures and an analysis of early gamma band phase locking in

schizophrenia," *Schizophrenia bulletin,* vol. 34, no. 5, pp. 907-926, 2008.

[7] J. Zheng, T. Su, L. Zhang, W. Zhu, and Q. H. Liu, "ISAR imaging of targets with complex motion based on the chirp rate–quadratic chirp rate distribution," *IEEE Transactions on Geoscience and Remote Sensing,* vol. 52, no. 11, pp. 7276-7289, 2014.

[8] F. Berizzi, E. D. Mese, M. Diani, and M. Martorella, "High-resolution ISAR imaging of maneuvering targets by means of the range instantaneous Doppler technique: Modeling and performance analysis," *IEEE Transactions on Image Processing,* vol. 10, no. 12, pp. 1880-1890, 2001.

[9] I. Djurović, M. Simeunović, and P. Wang, "Cubic phase function: A simple solution to polynomial phase signal analysis," *Signal Processing,* vol. 135, pp. 48-66, 2017.

[10] Y. Zhang, M. G. Amin, and G. J. Frazer, "High-resolution time–frequency distributions for manoeuvring target detection in over-the-horizon radars," *IEE Proceedings-Radar, Sonar and Navigation,* vol. 150, no. 4, pp. 299-304, 2003.

[11] I. Djurović, M. Simeunović, and B. Lutovac, "Are genetic algorithms useful for the parameter estimation of FM signals?," *Digital Signal Processing,* vol. 22, no. 6, pp. 1137-1144, 2012.

[12] B. J. Slocumb and J. Kitchen, "A polynomial phase parameter estimation-phase unwrapping algorithm," in *Proceedings of ICASSP'94. IEEE International Conference on Acoustics, Speech and Signal Processing*, 1994, vol. 4, pp. IV/129-IV/132 vol. 4: IEEE.

[13] X. Jiang, "Parameter Estimation of Polynomial Phase Signals Using Spectrum Distinction," *IEEE Transactions on Aerospace and Electronic Systems,* 2023.

[14] B. Porat and B. Friedlander, "Asymptotic statistical analysis of the high-order ambiguity function for parameter estimation of polynomial-phase signals," *IEEE Transactions on Information Theory,* vol. 42, no. 3, pp. 995-1001, 1996.

[15] S. Peleg and B. Porat, "Estimation and classification of polynomial-phase signals," *IEEE Transactions on Information Theory,* vol. 37, no. 2, pp. 422-430, 1991.

[16] S. Barbarossa, A. Scaglione, and G. B. Giannakis, "Product high-order ambiguity function for multicomponent polynomial-phase signal modeling," *IEEE Transactions on Signal Processing,* vol. 46, no. 3, pp. 691-708, 1998.

[17] M. Farquharson, P. O'Shea, and G. Ledwich, "A computationally efficient technique for estimating the parameters of polynomial-phase signals from noisy observations," *IEEE Transactions on Signal Processing,* vol. 53, no. 8, pp. 3337-3342, 2005.

[18] I. Djurovic, M. Simeunovic, S. Djukanovic, and P. Wang, "A hybrid CPF-HAF estimation of polynomial-phase signals: Detailed statistical analysis," *IEEE Transactions on Signal Processing,* vol. 60, no. 10, pp. 5010-5023, 2012.

[19] I. Djurović and L. Stanković, "Quasi-maximum-likelihood estimator of polynomial phase signals," *IET Signal Processing,* vol. 8, no. 4, pp. 347-359, 2014.

[20] I. Djurović, "On parameters of the QML PPS estimator," *Signal Processing,* vol. 116, pp. 1-6, 2015.

[21] I. Djurović and M. Simeunović, "Review of the quasi-maximum likelihood estimator for polynomial phase signals," *Digital Signal Processing,* vol. 72, pp. 59-74, 2018.

[22] Hatamian, A., Farshidi, F., Ghobadi, C., Nourinia, J. and Mostafapour, E., "Improving the quality of ecg signal using wavelet transform and adaptive filters", *Journal of Applied Research in Electrical Engineering,* vol. 2, no. 1, pp. 45-53, 2023.

[23] Amjadipour, F., Imani, M. and Ghassemian, H., "Morphological and Statistical Filter-Based Multi-Direction Building Detection for SAR Images", *Journal of Applied Research in Electrical Engineering*, vol. 2, no. 2, pp.145-151, 2023.

[24] A. K. Roonizi and I. W. Selesnick, "A Kalman Filter Framework for Simultaneous LTI Filtering and Total Variation Denoising," *IEEE Transactions on Signal Processing,* vol. 70, pp. 4543-4554, 2022.

[25] S. M. Kay, *Fundamentals of statistical signal processing: estimation theory*. Prentice-Hall, Inc., 1993.

[26] S.R. Samareh Hashemi, "Enhancement of phase unwrapping algorithm using a prediction filter for estimating the parameters of polynomial phase signals," (in Persian), in *7th Iranian national conference on radar and surveillance systems*, Tehran, Iran, 2020.

[27] P. O'Shea, "On refining polynomial phase signal parameter estimates," *IEEE Transactions on Aerospace and Electronic Systems,* vol. 46, no. 3, pp. 978-987, 2010.

BIOGRAPHY



Seyed Rouhollah Samareh Hashemi received the B.Sc, M.Sc and PhD degrees in electrical enginering from the Sharif University of Thechnology, Tehran, Iran (2002), Shahid Beheshti University, Tehran, Iran (2005) and Ferdowsi University of Mashhad, Mashhad, Iran (2015) respectively. He is currenly an assistant professor at the photonics research institute, Graduate University of Advanced Technology, Kerman, Iran. His research interests include signal processing and radar imaging.



Fatemeh Hatami was born in 1997 in Kerman, Iran. She is currently a PhD. student in electrical engineering, (communication systems) at the Graduate University of Advanced Technology, Kerman, Iran. Her research interests include signal processing and radar systems, particularly Synthetic Aperture Radar (SAR).

Copyrights
© 2026 by the author(s). Licensee Shahid Chamran University of Ahvaz, Ahvaz, Iran. This article is an open-access article distributed under the terms and conditions of the Creative Commons Attribution –NonCommercial 4.0 International (CC BY-NC 4.0) License (http://creativecommons.org/licenses/by-nc/4.0/).